Journal of Sound and Vibration (2000) **230**(1), 111–132
doi:10.1006/jsvi.1999.2612, available online at http://www.idealibrary.com on IDEAL®

FREE VIBRATION OF SYMMETRICALLY LAMINATED THICK-PERFORATED PLATES

C. C. CHEN AND S. KITIPORNCHAI

Department of Civil Engineering, The University of Queensland, Brisbane, Queensland 4072, *Australia*

C. W. LIM

Department of Mechanical Engineering, The University of Hong Kong, Hong Kong

AND

K. M. LIEW

Centre for Advanced Numerical Engineering Simulations (*CANES*), *School of Mechanical and Production Engineering, Nanyang Technological University, Singapore* 639798, *Singapore*

(*Received* 3 *February* 1999, *and in final form* 21 *August* 1999)

This paper investigates the free vibration of symmetrically laminated, thick, doubly connected plates of arbitray plate perimeter for the outer boundary and a hole defined by a super-elliptical equation which is able to describe a rectangle, ellipse or quasi-rectangle. The laminated perforated plates can be subject to free, simply supported, or clamped edge conditions. Convergence and comparisons with established work have been studied to ensure accuracy of results. Efforts are made to interpret the frequency results to provide physical insight to the problem.

1. INTRODUCTION

The free vibration of laminated composite plates has been extensively analyzed for a wide range of applications varying from general civil or mechanical engineering to more specific aerospace or marine engineering. The primary advantage of laminated structures is that the stiffness and strength can be aligned in any desired direction. However, the use of conventional thin plates has found limitations in applications such as underwater marine structures, military combat vehicles and nuclear power plant installations. These applications require relatively thick plate assemblies to sustain enormous internal and external pressure or loading. Further, laminates with concentric or eccentric holes, which lead to more complicated analysis, are commonly seen in industrial practice. As a result, the complicated analysis of laminated, thick, perforated plates poses a tremendous challenge for researchers.

Investigations on this subject have been confined to thin, isotropic, perforated plates using the Fourier expansion collocation method [1–4], Rayleigh–Ritz

0022-460X/00/060111 + 22 $35.00/0

method [5, 6], finite element method [7], other specific methods [8, 9], and experimental studies [3, 4, 9]. Research devoted to the vibrational analysis for perforated laminates is very limited. Rajamani and Prabhakaran [10, 11] assumed the effect of the cutouts was equivalent to an external loading on the plate and investigated the dynamic response of thin, simply supported and clamped, square laminates with coincident circular or square cutouts. Liew [12] and Lim and Liew [13] analyzed the free vibration of doubly connected, thin, super-elliptical laminates by assuming a set of admissible polynomial shape functions for the Rayleigh–Ritz method. However, it is well known that classical laminate theory is insufficient for the analysis of laminates with a lower length- or width-to-thickness ratio, which practically cannot be less than 50.

For laminates with lower length-to-thickness ratio, the first order laminate theory introduced by Yang *et al.* [14] relaxes the Kirchhoff–Love assumption but introduces a contradictory shear correction factor which depends on many factors in the lamination and is not known for arbitrary composite laminates. This requirement for shear correction factors in the first order shear deformation theory has made it less attractive for laminates. In the early 1980s, Reddy [15] proposed a higher order shear deformation theory to eradicate the artificial shear correction factor and to satisfy the strain-free condition on the top and bottom plate surfaces. The higher order plate model has since gained much popularity due to its superiority and elimination of shear correction factor. More accurate laminate theories such as three-dimensional (3-D) elasticity and layerwise theories require expensive computation effort, thus preventing their general use in modelling an entire laminated structure. Therefore, the higher order shear deformation theory is good choice for determination of the global response of thicker structures.

More recently, researchers have focused on the problems of isotropic thick plates or laminates with concentric circular or elliptical holes. Bicos and Springer [16, 17] applied Reddy's higher order theory [15] and finite element methods for the free damped and undamped vibration of laminated composite plates and shells with a concentric circular hole. Ramkrishna *et al.* [18] used an eight-noded hybrid-stress isoparametric finite element for the free vibration analysis of simply supported laminates with a concentric elliptical hole. Young *et al.* [19] presented a Rayleigh–Ritz approach using the three-dimensional elasticity theory for the analysis of the free vibration of isotropic, thick, rectangular plates, with depressions, grooves, or cutouts. In the context of laminated thick plates, however, due to the complexity of formulation for the higher order plate model, the authors have not located any investigations on the free vibration of thick laminated perforated plates with various outer and inner perimeters.

The authors present the first attempt to examine the vibration of symmetrically laminated, thick, perforated plates using Rayleigh–Ritz method and Reddy's higher order theory. The outer periphery is not only confined to a rectangular planform but also more general shapes including circle, ellipse, super-ellipse, and trapezoids. Accordingly, the hole can be either concentric or eccentric circular, elliptical, or rectangular cutout. In this investigation, the authors further extend the use of polynomial shape functions developed in previous work [12, 13] to thick laminated perforated plates. Specific shape functions are superior to, and more versatile than,

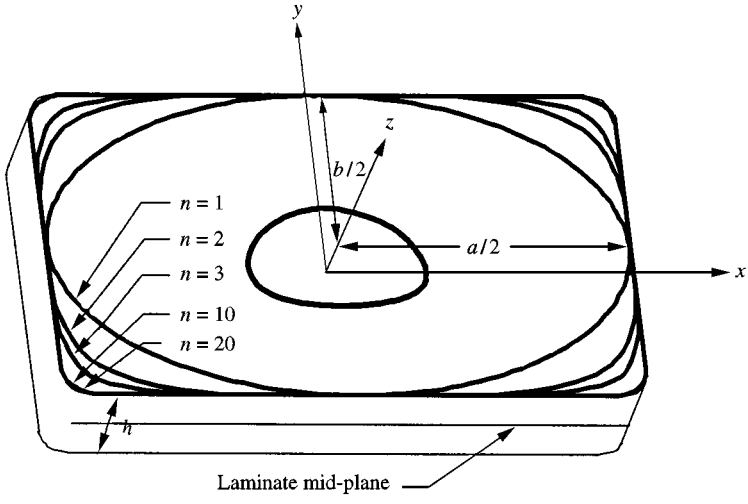

Figure 1. Geometric definitions of a super-elliptical laminated plate with a hole.

the conventional trigonometric shape functions. All free, simply supported and clamped boundary constraints can be satisfied at the outset because these conditions are implicit in the shape functions and controlled by a basic power. Effects of lamination layup, length-to-thickness ratios, aspect ratios, stacking angles, cutout geometry and boundary condition have been examined.

2. MATHEMATICAL FORMULATION

A flat, symmetrically laminated, thick, perforated plate is considered. The reference Cartesian co-ordinate system is located in the middle of the laminated plates as illustrated in Figure 1. The laminae are assumed to be perfectly bonded together and possess a plane of elastic symmetry parallel to the xy plane.

The total kinetic energy T for the laminated plate consisting of N orthotropic laminae, in the presence of free vibration, has the following form:

$$T = \frac{h}{2} \sum_{k=1}^{N} \int\int_{A} \rho_k \left[\left(\frac{\partial u}{\partial t} \right)^2 + \left(\frac{\partial v}{\partial t} \right)^2 + \left(\frac{\partial w}{\partial t} \right)^2 \right] \mathrm{d}A, \tag{1}$$

in which h is the total thickness of the laminated plate, and A and ρ_k are area and mass density of the kth lamina respectively. u, v, and w are the in-plane and out-of-plane displacement components of a general point of the laminated plate.

Neglecting the effect of transverse normal stress σ_z, one can express the total strain energy for the laminated plate as

$$U = \frac{1}{2} \sum_{k=1}^{N} \int\int_{A} \int_{h_{k-1}}^{h_k} (\sigma_x \varepsilon_x + \sigma_y \varepsilon_y + \sigma_{xz} \varepsilon_{xz} + \sigma_{yz} \varepsilon_{yz} + \sigma_{xy} \varepsilon_{xy})_k \, \mathrm{d}z \, \mathrm{d}A. \tag{2}$$

Also, the displacement field of laminated plate based on Reddy's higher order shear deformation theory is

$$u(x,y,z,t) = u_0(x,y,t) + z\phi_x(x,y,t) + z^3\left(-\frac{4}{3h^2}\right)\left(\phi_x(x,y,t) + \frac{\partial w(x,y,t)}{\partial x}\right),$$

$$v(x,y,z,t) = v_0(x,y,t) + z\phi_y(x,y,t) + z^3\left(-\frac{4}{3h^2}\right)\left(\phi_y(x,y,t) + \frac{\partial w(x,y,t)}{\partial y}\right),$$

$$w(x,y,z,t) = w_0(x,y,t), \tag{3}$$

where u_0, v_0, w_0, ϕ_x, and ϕ_y are the displacement and rotation components of the mid-plane of the laminated plate in the Cartesian co-ordinate respectively. Further, one can decouple the variable t and the components u_0, v_0, w_0, ϕ_x, and ϕ_y by assuming small-amplitude vibration and rewrite the components in equation (1) in sinusoidal form as

$$u_0(x,y,t) = U(x,y)\sin\omega t,$$

$$v_0(x,y,t) = V(x,y)\sin\omega t,$$

$$w_0(x,y,t) = W(x,y)\sin\omega t,$$

$$\phi_x(x,y,t) = \Theta_u(x,y)\sin\omega t,$$

$$\phi_y(x,y,t) = \Theta_v(x,y)\sin\omega t. \tag{4}$$

Substituting equation (4) into equations (1)–(3), the maximum strain energy $U_{\max}$ and the maximum kinetic energy $T_{\max}$ during a vibratory cycle can be determined. For a non-dissipative system, the total strain energy and the total kinetic energy corresponding to the free vibration are equal. The governing equation for the free vibration of laminated plate can then be established by using the Rayleigh–Ritz method to minimize the following governing total energy functional:

$$\Pi = U_{\max} - T_{\max}. \tag{5}$$

The Rayleigh–Ritz method requires the solution in the form of a series containing unknown parameters. Therefore, a finite set of unknown parameters have been introduced in the non-dimensional displacement and rotation function,

$$U(\xi,\eta) = \sum_{i=1}^{m} c_i^u \varphi_i^u(\xi,\eta),$$

$$V(\xi,\eta) = \sum_{i=1}^{m} c_i^v \varphi_i^v(\xi,\eta),$$

$$W(\xi,\eta) = \sum_{i=1}^{m} c_i^w \varphi_i^w(\xi,\eta),$$

$$\Theta_u(\xi,\eta) = \sum_{i=1}^{m} c_i^{\theta_u} \varphi_i^{\theta_u}(\xi,\eta),$$

$$\Theta_v(\xi,\eta) = \sum_{i=1}^{m} c_i^{\theta_v} \varphi_i^{\theta_v}(\xi,\eta), \tag{6}$$

where φ_i^u, φ_i^v, φ_i^w, $\varphi_i^{\theta_u}$, and $\varphi_i^{\theta_v}$ are the shape functions and c_i^u, c_i^v, c_i^w, $c_i^{\theta_u}$, and $c_i^{\theta_v}$ are the associated unknown coefficients. ξ and η denote the non-dimensional co-ordinates given by

$$\xi = x/a, \qquad \eta = y/b, \tag{7}$$

where a and b are width and length of the laminated plate.

The problem now lies in finding suitable shape functions that are general for any boundary conditions and plate geometries. Liew and Wang [20] proposed a strategy known as the p-Ritz method for generating a set of shape functions which satisfy the boundary conditions by embedding the basic functions. In the p-Ritz method, the shape functions, φ_i^u, φ_i^v, φ_i^w, $\varphi_i^{\theta_u}$, and $\varphi_i^{\theta_v}$ are assumed to be the products of two-dimensional polynomials and basic functions as follows:

$$\varphi_i^\kappa(\xi,\eta) = f_i(\xi,\eta)\,\varphi_b^\kappa(\xi,\eta), \tag{8}$$

in which $\kappa = u, v, w, \theta_u, \theta_v$. $\varphi_b^\kappa(\xi,\eta)$ is the basic function which is assumed to be the product of boundary expressions of all supporting edges. For instance, the basic function, for the perforated laminated plate, can be assumed as

$$\varphi_b^\kappa(\xi,\eta) = \varphi_b^{\kappa_1}\,\varphi_b^{\kappa_2}. \tag{9}$$

Here, $\varphi_b^{\kappa_1}$ *and* $\varphi_b^{\kappa_2}$ are the basic functions for the outer and inner boundaries of the perforated laminated plate, respectively. In this study, the periphery of the laminated perforated plate is assumed to be a super-ellipse or a trapezoid while the perimeter of the hole is a super-ellipse. If the outer perimeter of the perforated laminated plate is a super-ellipse, we have the non-dimensional basic function

$$\varphi_b^{\kappa_1} = [(2\xi)^{2n_1} + (2\eta)^{2n_1} - 1]^{\Omega^{\kappa_1}} \tag{10}$$

where n_1 and Ω^{κ_1} represent the super-elliptical power and associated basic power for the outer boundary respectively. The basic power Ω^κ ensures automatic satisfaction of the boundary condition for the outer supporting edge. It is assigned different values depending on the edge constraint. Here are general rules for

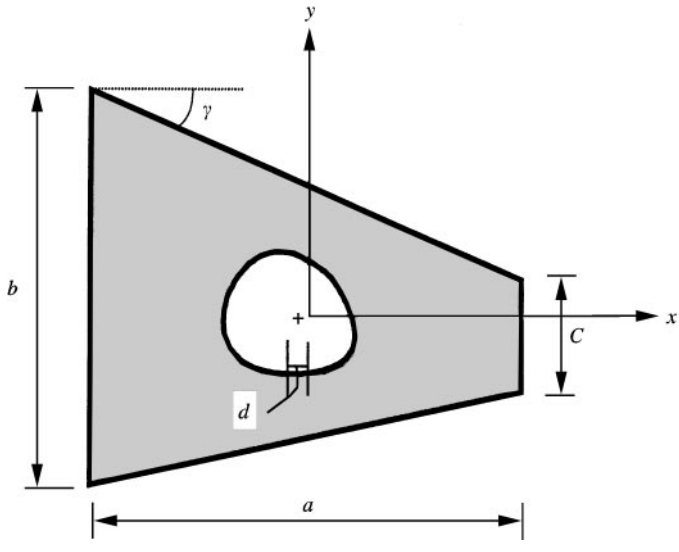

Figure 2. Plane view of trapezoidal laminated perforated plates.

defining the basic power:

- For the sth edge subject to free constraint, we have

$$\Omega_s^u = \Omega_s^v = \Omega_s^w = \Omega_s^{\theta_u} = \Omega_s^{\theta_v} = 0. \tag{11}$$

- If subject to simply supported constraint then only the w direction is constrained,

$$\Omega_s^u = \Omega_s^v = \Omega_s^{\theta_u} = \Omega_s^{\theta_v} = 0, \qquad \Omega_s^w = 1. \tag{12}$$

- Or with clamped constraint,

$$\Omega_s^u = \Omega_s^v = \Omega_s^{\theta_u} = \Omega_s^{\theta_v} = 1, \qquad \Omega_s^w = 2. \tag{13}$$

For a trapezoidal laminated perforated plate as shown in Figure 2, the basic function for the trapezoid is given by the product of boundary equations of all supporting edges, that is,

$$\varphi_b^{\kappa_1} = \left(\xi + \frac{1}{2}\right)^{\Omega_1^{\kappa_1}} \left\{\eta + \left[\frac{a}{b}\tan\gamma - 1 + \frac{c}{b}\right]\xi + \frac{1}{4}\left(1 + \frac{c}{b}\right)\right\}^{\Omega_2^{\kappa_1}} \left(\xi - \frac{1}{2}\right)^{\Omega_3^{\kappa_1}} \times \left\{\eta + \xi\frac{a}{b}\tan\gamma - \frac{1}{4}\left(1 + \frac{c}{b}\right)\right\}^{\Omega_4^{\kappa_1}}, \tag{14}$$

in which $\kappa_1 = u, v, w, \theta_u, \theta_v, a/b$ is the aspect ratio, and c/b is the taper ratio. c is the length of the edge along $x = a/2$, γ is the degree of skewness of the trapezoids and

measures positive in the clockwise direction. Edge 1 refers to the edge at $x = -a/2$ and 2, 3, 4 correspond to the subsequent edges, going counteclockwise.

Similarly, the basic function for the eccentric hole shown in Figure 2 is of the form

$$\varphi_b^{\kappa_2} = \left[\left(\frac{2a\xi - 2d}{a'} \right)^{2n_2} + \left(\frac{2b\eta}{b'} \right)^{2n_2} - 1 \right]^{\Omega^{\kappa_2}}, \tag{15}$$

where n_2 and Ω^{κ_2} represent the super-elliptical power and associated basic power for the internal boundary respectively, d is the distance in the x direction between centers of inner and outer boundaries. a' and b' are width and length of the hole respectively.

The function $f_i(\xi, \eta)$ can be constructed using a two-dimensional polynomial series

$$\sum_{i=1}^{m} f_i(\xi, \eta) = \sum_{q=0}^{p} \sum_{i=0}^{q} \xi^{q-i} \eta^i, \tag{16}$$

where p is the highest degree of the set of two-dimensional polynomials.

Substituting equations (6) and (8) into equation (5) and minimizing the total energy functional Π with respect to the unknown coefficients yield the governing eigenvalue equation

$$\{[K] - \lambda^2 [M]\}\{c\} = \{0\}, \tag{17}$$

where $\{c\} = \{c^u \quad c^v \quad c^w \quad ac^{\theta_u}, \; bc^{\theta_v}\}^{\mathrm{T}}$.

If all laminae are made of the same material, the non-dimensional frequency parameter λ can be expressed in terms of frequency, plate dimensions, D_0, and mass density per unit volume ρ as

$$\lambda = \omega ab \sqrt{\frac{\rho h}{D_0}}, \tag{18}$$

where

$$D_0 = \frac{E_{11} h^3}{12(1 - v_{12} v_{21})}. \tag{19}$$

In equation (19), E_{11} denotes the Young's moduli in the 1–1 direction of the material plane, and v_{12} and v_{21} represent the Poisson ratios along the 1–2 and 2–1 directions respectively.

The vibration frequencies and mode shapes of perforated laminates are then obtained by solving λ. Details of the stiffness and mass matrices $[K]$ and $[M]$ in

equation (17) are given by

$$[K] = \frac{1}{D_0}\begin{bmatrix} [K^{uu}] & [K^{uv}] & 0 & 0 & 0 \\ & [K^{vv}] & 0 & 0 & 0 \\ & & [K^{ww}] & [K^{w\theta_u}] & [K^{w\theta_v}] \\ & sym. & & [K^{\theta_u\theta_u}] & [K^{\theta_u\theta_v}] \\ & & & & [K^{\theta_v\theta_v}] \end{bmatrix}, \tag{20}$$

and

$$[M] = \begin{bmatrix} [M^{uu}] & 0 & 0 & 0 & 0 \\ & [M^{vv}] & 0 & 0 & 0 \\ & & [M^{ww}] & [M^{w\theta_u}] & [M^{w\theta_v}] \\ & sym. & & [M^{\theta_u\theta_u}] & 0 \\ & & & & [M^{\theta_v\theta_v}] \end{bmatrix}. \tag{21}$$

More explicitly, the elements of K can be expressed as

$$K_{ij}^{uu} = A_{66}\left(\frac{a^2}{h^3}\right)R_{\varphi_i^u\varphi_j^u}^{0101} + A_{16}\left(\frac{ab}{h^3}\right)[R_{\varphi_i^u\varphi_j^u}^{0110} + R_{\varphi_i^u\varphi_j^u}^{1001}] + A_{11}\left(\frac{b^2}{h^3}\right)R_{\varphi_i^u\varphi_j^u}^{1010},$$

$$K_{ij}^{uv} = A_{26}\left(\frac{a^2}{h^3}\right)R_{\varphi_i^v\varphi_j^u}^{0101} + \left(\frac{ab}{h^3}\right)[A_{66}R_{\varphi_i^u\varphi_j^v}^{0110} + A_{12}R_{\varphi_i^u\varphi_j^v}^{1001}] + A_{16}\left(\frac{b^2}{h^3}\right)R_{\varphi_i^u\varphi_j^v}^{1010},$$

$$K_{ij}^{vv} = A_{22}\left(\frac{a^2}{h^3}\right)R_{\varphi_i^v\varphi_j^v}^{0101} + A_{26}\left(\frac{ab}{h^3}\right)[R_{\varphi_i^v\varphi_j^v}^{0110} + R_{\varphi_i^v\varphi_j^v}^{1001}] + A_{66}\left(\frac{b^2}{h^3}\right)R_{\varphi_i^v\varphi_j^v}^{1010},$$

$$\begin{aligned} K_{ij}^{ww} = {} & \left[A_{44}\left(\frac{a^2}{h^3}\right) - D_{44}\left(\frac{8a^2}{h^5}\right) + F_{44}\left(\frac{16a^2}{h^7}\right)\right]R_{\varphi_i^w\varphi_j^w}^{0101} + \left[A_{45}\left(\frac{ab}{h^3}\right)\right. \\ & \left. - D_{45}\left(\frac{8ab}{h^5}\right) + F_{45}\left(\frac{16ab}{h^7}\right)\right][R_{\varphi_i^w\varphi_j^w}^{0110} + R_{\varphi_i^w\varphi_j^w}^{1001}] + \left[A_{55}\left(\frac{b^2}{h^3}\right) - D_{55}\left(\frac{8b^2}{h^5}\right)\right. \\ & \left. + F_{55}\left(\frac{16b^2}{h^7}\right)\right]R_{\varphi_i^w\varphi_j^w}^{1010} + H_{22}\left(\frac{16a^2}{9b^2h^7}\right)R_{\varphi_i^w\varphi_j^w}^{0202} + H_{26}\left(\frac{32a}{9bh^7}\right)[R_{\varphi_i^w\varphi_j^w}^{0211} \\ & + R_{\varphi_i^w\varphi_j^w}^{1102}] + H_{66}\left(\frac{64}{9h^7}\right)R_{\varphi_i^w\varphi_j^w}^{1111} + H_{16}\left(\frac{32b}{9ah^7}\right)[R_{\varphi_i^w\varphi_j^w}^{1120} + R_{\varphi_i^w\varphi_j^w}^{2011}] \\ & + H_{12}\left(\frac{16}{9h^7}\right)[R_{\varphi_i^w\varphi_j^w}^{0220} + R_{\varphi_i^w\varphi_j^w}^{2002}] + H_{11}\left(\frac{16b^2}{9a^2h^7}\right)R_{\varphi_i^u\varphi_j^u}^{2020}, \end{aligned}$$

$$K_{ij}^{w\theta_u} = \left[A_{45}\left(\frac{ab}{h^3}\right) - D_{45}\left(\frac{8ab}{h^5}\right) + F_{45}\left(\frac{16ab}{h^7}\right)\right] R^{0100}_{\varphi_i^w \varphi_j^{\theta_u}} + \left[H_{26}\left(\frac{16a}{9bh^7}\right)\right.$$

$$\left. - F_{26}\left(\frac{4a}{3bh^5}\right)\right] R^{0201}_{\varphi_i^w \varphi_j^{\theta_u}} + \left[H_{12}\left(\frac{16}{9h^7}\right) - F_{12}\left(\frac{4}{3h^5}\right)\right)\right] R^{0210}_{\varphi_i^w \varphi_j^{\theta_u}} + \left[A_{55}\left(\frac{b^2}{h^3}\right)\right.$$

$$\left. - D_{55}\left(\frac{8b^2}{h^5}\right) + F_{55}\left(\frac{16b^2}{h^7}\right)\right] R^{1000}_{\varphi_i^w \varphi_j^{\theta_u}} + \left[H_{66}\left(\frac{32}{9h^7}\right) - F_{66}\left(\frac{8}{3h^5}\right)\right] R^{1101}_{\varphi_i^w \varphi_j^{\theta_u}}$$

$$+ \left[H_{16}\left(\frac{16b}{9ah^7}\right) - F_{16}\left(\frac{4b}{3ah^5}\right)\right] [2R^{1110}_{\varphi_i^w \varphi_j^{\theta_u}} + R^{2001}_{\varphi_i^w \varphi_j^{\theta_u}}] + \left[H_{11}\left(\frac{16b^2}{9a^2h^7}\right)\right.$$

$$\left. - F_{11}\left(\frac{4b^2}{3a^2h^5}\right)\right] R^{2010}_{\varphi_i^w \varphi_j^{\theta_u}},$$

$$K_{ij}^{w\theta_v} = \left[A_{44}\left(\frac{a^2}{h^3}\right) - D_{44}\left(\frac{8a^2}{h^5}\right) + F_{44}\left(\frac{16a^2}{h^7}\right)\right] R^{0100}_{\varphi_i^w \varphi_j^{\theta_v}} + \left[H_{22}\left(\frac{16a^2}{9b^2h^7}\right)\right.$$

$$\left. - F_{22}\left(\frac{4a^2}{3b^2h^5}\right)\right] R^{0201}_{\varphi_i^w \varphi_j^{\theta_v}} + \left[H_{26}\left(\frac{16a}{9bh^7}\right) - F_{26}\left(\frac{4a}{3bh^5}\right)\right] R^{0210}_{\varphi_i^w \varphi_j^{\theta_v}} + \left[A_{45}\left(\frac{ab}{h^3}\right)\right.$$

$$\left. - D_{45}\left(\frac{8ab}{h^5}\right) + F_{45}\left(\frac{16ab}{h^7}\right)\right] R^{1000}_{\varphi_i^w \varphi_j^{\theta_v}} + \left[H_{26}\left(\frac{32a}{9bh^7}\right) - F_{26}\left(\frac{8a}{3bh^5}\right)\right] R^{1101}_{\varphi_i^w \varphi_j^{\theta_v}}$$

$$+ \left[H_{66}\left(\frac{32}{9h^7}\right) - F_{66}\left(\frac{8}{3h^5}\right)\right] R^{1110}_{\varphi_i^w \varphi_j^{\theta_v}} + \left[H_{12}\left(\frac{16}{9h^7}\right) - F_{12}\left(\frac{4}{3h^5}\right)\right] R^{2001}_{\varphi_i^w \varphi_j^{\theta_v}}$$

$$+ \left[H_{16}\left(\frac{16b}{9ah^7}\right) - F_{16}\left(\frac{4b}{3ah^5}\right)\right] R^{2010}_{\varphi_i^w \varphi_j^{\theta_v}},$$

$$K_{ij}^{\theta_u \theta_u} = \left[A_{55}\left(\frac{b^2}{h^3}\right) - D_{55}\left(\frac{8b^2}{h^5}\right) + F_{55}\left(\frac{16b^2}{h^7}\right)\right] R^{0000}_{\varphi_i^{\theta_u} \varphi_j^{\theta_u}} + \left[D_{66}\left(\frac{1}{h^3}\right)\right.$$

$$\left. + H_{66}\left(\frac{16}{9h^7}\right) - F_{66}\left(\frac{8}{3h^5}\right)\right] R^{0101}_{\varphi_i^{\theta_u} \varphi_j^{\theta_u}} + \left[D_{16}\left(\frac{b}{ah^3}\right) + H_{16}\left(\frac{16b}{9ah^7}\right)\right.$$

$$\left. - F_{16}\left(\frac{8b}{3ah^5}\right)\right] [R^{0110}_{\varphi_i^{\theta_u} \varphi_j^{\theta_u}} + R^{1001}_{\varphi_i^{\theta_u} \varphi_j^{\theta_u}}] + \left[D_{11}\left(\frac{b^2}{a^2h^3}\right) + H_{11}\left(\frac{16b^2}{9a^2h^7}\right)\right.$$

$$\left. - F_{11}\left(\frac{8b^2}{3a^2h^5}\right)\right] R^{1010}_{\varphi_i^{\theta_u} \varphi_j^{\theta_u}},$$

$$K_{ij}^{\theta_u\theta_v} = \left[A_{45}\left(\frac{ab}{h^3}\right) - D_{45}\left(\frac{8ab}{h^5}\right) + F_{45}\left(\frac{16ab}{h^7}\right)\right] R^{0000}_{\varphi_i^{\theta_u}\varphi_j^{\theta_v}} + \left[D_{26}\left(\frac{a}{bh^3}\right) + H_{26}\left(\frac{16a}{9bh^7}\right) - F_{26}\left(\frac{8a}{3bh^5}\right)\right] R^{0101}_{\varphi_i^{\theta_u}\varphi_j^{\theta_v}} + \left[D_{66}\left(\frac{1}{h^3}\right) + H_{66}\left(\frac{16}{9h^7}\right) - F_{66}\left(\frac{8}{3h^5}\right)\right] R^{0110}_{\varphi_i^{\theta_u}\varphi_j^{\theta_v}} + \left[D_{12}\left(\frac{1}{h^3}\right) + H_{12}\left(\frac{16}{9h^7}\right) - F_{12}\left(\frac{8}{3h^5}\right)\right] R^{1001}_{\varphi_i^{\theta_u}\varphi_j^{\theta_v}} + \left[D_{16}\left(\frac{b}{ah^3}\right) + H_{16}\left(\frac{16b}{9ah^7}\right) - F_{16}\left(\frac{8b}{3ah^5}\right)\right] R^{1010}_{\varphi_i^{\theta_u}\varphi_j^{\theta_v}},$$

$$K_{ij}^{\theta_v\theta_v} = \left[A_{44}\left(\frac{a^2}{h^3}\right) - D_{44}\left(\frac{8a^2}{h^5}\right) + F_{44}\left(\frac{16a^2}{h^7}\right)\right] R^{0000}_{\varphi_i^{\theta_v}\varphi_j^{\theta_v}} + \left[D_{22}\left(\frac{a^2}{b^2h^3}\right) + H_{22}\left(\frac{16a^2}{9b^2h^7}\right) - F_{22}\left(\frac{8a^2}{3b^2h^5}\right)\right] R^{0101}_{\varphi_i^{\theta_v}\varphi_j^{\theta_v}} + \left[D_{26}\left(\frac{a}{bh^3}\right) + H_{26}\left(\frac{16a}{9bh^7}\right) - F_{26}\left(\frac{8a}{3bh^5}\right)\right] [R^{1010}_{\varphi_i^{\theta_v}\varphi_j^{\theta_v}} + R^{1001}_{\varphi_i^{\theta_v}\varphi_j^{\theta_v}}] + \left[D_{66}\left(\frac{1}{h^3}\right) + H_{66}\left(\frac{16}{9h^7}\right) - F_{66}\left(\frac{8}{3h^5}\right)\right] R^{1010}_{\varphi_i^{\theta_v}\varphi_j^{\theta_v}}. \tag{22}$$

Accordingly, the elements in $[M]$ can be further expanded as

$$M_{ij}^{uu} = hR^{0000}_{\varphi_i^u\,\varphi_j^u},$$

$$M_{ij}^{vv} = hR^{0000}_{\varphi_i^v\,\varphi_j^v},$$

$$M_{ij}^{ww} = hR^{0000}_{\varphi_i^w\,\varphi_j^w} + \left(\frac{h^3}{252b^2}\right) R^{0101}_{\varphi_i^w\,\varphi_j^w} + \left(\frac{h^3}{252a^2}\right) R^{1010}_{\varphi_i^w\,\varphi_j^w},$$

$$M_{ij}^{w\theta_u} = \left(\frac{-4h^3}{315a^2}\right) R^{1000}_{\varphi_i^w\,\varphi_j^{\theta_u}},$$

$$M_{ij}^{w\theta_v} = \left(\frac{-4h^3}{315b^2}\right) R^{0100}_{\varphi_i^w\,\varphi_j^{\theta_v}},$$

$$M_{ij}^{\theta_u\theta_u} = \left(\frac{17h^3}{315a^2}\right) R^{0000}_{\varphi_i^{\theta_u}\varphi_j^{\theta_u}},$$

$$M_{ij}^{\theta_v\theta_v} = \left(\frac{17h^3}{315b^2}\right) R^{0000}_{\varphi_i^{\theta_v}\varphi_j^{\theta_v}}, \tag{23}$$

where

$$R^{defg}_{\varphi_i^\alpha \theta_j^\beta} = \int\int_A \frac{\partial^{d+e} \varphi_i^\alpha(\xi,\eta)}{\partial \xi^d \partial \eta^e} \frac{\partial^{f+g} \theta_j^\beta(\xi,\eta)}{\partial \xi^f \partial \eta^g} \, d\xi \, d\eta, \tag{24}$$

in which $\varphi^\alpha, \theta^\beta = \varphi^u, \varphi^v, \varphi^w, \varphi^{\theta_u}, \varphi^{\theta_v}$ and $i, j = 1, 2, \ldots, m$. In addition, the integrand R in equation (24) is obtained by the Gaussian quadrature method.

3. NUMERICAL STUDIES AND DISCUSSIONS

The verification of the aforementioned method has been carried out by solving many examples of symmetrically laminated, thick, perforated plates. The laminae of the plate are assumed to have the same thickness. In the subsequent analysis, three materials with the properties given below have been studied:

Material 1: $E_1/E_2 = 40$, $G_{12}/E_2 = 0{\cdot}6$, $G_{23}/E_2 = 0{\cdot}5$, $G_{13} = G_{12}$, and $\nu_{12} = 0{\cdot}25$,

Material 2: $E_1/E_2 = 1{\cdot}0$, $G_{12}/E_2 = 1/2(1+\nu)$, $G_{23} = G_{13} = G_{12}$, $\nu = 0{\cdot}3$,

Material 3: $E_1 = 60{\cdot}7\,\text{GPa}$, $E_2 = 24{\cdot}8\,\text{GPa}$, $G_{12} = G_{23} = G_{13} = 12\,\text{GPa}$, $\nu_{12} = 0{\cdot}23$,

Material 4: $E_1 = 130\,\text{GPa}$, $E_2 = 9\,\text{GPa}$, $G_{12} = G_{23} = G_{13} = 4{\cdot}8\,\text{GPa}$, $\nu_{12} = 0{\cdot}28$.

Materials 1 and 2 were selected for historical reasons because they have been widely used in many previous investigations. Materials 3 and 4 represent E-glass/epoxy and carbon fiber/epoxy respectively, which are two practical materials for composite laminates. As a convention for the boundary constraints, the notation for outer boundaries is generally placed in front of the one for the hole. For example, SF denotes simply supported at the periphery of laminates and free at the hole. Here, F, S, C stand for free, simply supported, and clamped respectively. This notation has been used throughout this paper.

The convergence studies for the degree of polynomials p on the frequency parameters have been performed and presented in Tables 1 and 2 to ensure that a sufficient number of terms are employed for the integration. In Table 1, we analyzed an eight-ply, elliptical laminates of Material 1 with a concentric square hole, $a/b = 2$, $a'/a = 0{\cdot}3$, $a/h = 5$, stacking sequence $[(\theta/-\theta)_2]_s$, and CF boundary condition. By increasing the degree of polynomial p from 8 to 15 in the assumed series, it is seen that the difference is less than 3·5% between the frequency parameters of $p = 13$ and 15 for all modes. The second example considers a cantilever trapezoidal laminated plate of Material 1, clamped at $x = -a/2$, with a free circular hole at the center, $a/b = 2$, $c/b = 0{\cdot}6$, $a'/a = 0{\cdot}3$, $a/h = 5$, and stacking sequence $[(\theta/-\theta)_2]_s$. The frequency results have been summarized in Table 2. It is found that convergence of the second example is faster than that of the first example with less than 0·3% difference between the frequencies of using $p = 13$ and 15 for all

TABLE 1

Convergence of degree of polynomials p on the frequency parameters λ of the clamped elliptical laminates with free concentric square hole ($a/b = 2$, $a'/a = 0{\cdot}3$, *and* $a/h = 5$)

		Mode sequence number							
θ	p	1	2	3	4	5	6	7	8
0	8	7·2308	8·8276	9·8521	11·6851	12·2011	13·1610	13·4303	15·1673
	11	7·2178	8·7588	9·7000	11·6751	12·1566	12·9562	13·3541	14·8820
	13	7·2140	8·7204	9·6493	11·6692	12·1246	12·8473	13·3179	14·8409
	14	7·2131	8·6996	9·6251	11·6639	12·1246	12·8158	13·3054	14·8409
	15	7·2117	8·6903	9·6172	11·6639	12·0943	12·7558	13·2913	14·8194
30	8	8·5924	9·6153	11·8042	13·7441	15·5212	17·0725	18·9197	19·9064
	11	8·5806	9·5825	11·6413	13·6342	15·4117	17·0572	18·7935	19·6106
	13	8·5740	9·5657	11·5557	13·5749	15·3579	17·0394	18·7120	19·5476
	14	8·5713	9·5545	11·5138	13·5612	15·3395	17·0293	18·6646	19·5344
	15	8·5684	9·5504	11·4950	13·5221	15·3150	17·0238	18·6501	19·4905
45	8	9·4107	10·1441	13·2988	14·1833	17·0263	17·0439	19·3934	20·1670
	11	9·3989	10·1201	13·0281	14·0826	16·8691	17·0266	19·1020	19·9938
	13	9·3937	10·1066	12·8553	14·0261	16·7888	17·0141	19·0470	19·8845
	14	9·3920	10·0981	12·7613	14·0139	16·7648	17·0102	19·0362	19·8167
	15	9·3886	10·0954	12·7306	14·9813	16·7182	17·0043	19·0033	19·7956
60	8	10·0706	10·5599	14·3476	14·7723	16·6591	18·2414	18·7442	21·2045
	11	10·0584	10·5404	14·2538	14·3043	16·6318	17·9853	18·4895	20·9845
	13	10·0539	10·5286	13·9743	14·2020	16·6185	17·8709	18·4180	20·8652
	14	10·0528	10·5213	13·7872	14·1920	16·6149	17·8388	18·4008	20·7929
	15	10·0495	10·5195	13·7340	14·1692	16·6099	17·7601	18·3670	20·7644
90	8	10·1567	10·7023	10·8617	11·4871	13·1485	13·4345	14·6209	16·0734
	11	10·1525	10·6718	10·8292	11·4420	13·0078	13·4160	14·5673	15·7930
	13	10·1498	10·6612	10·8099	11·4187	12·9731	13·4059	14·5303	15·1114
	14	10·1477	10·6583	10·7975	11·4187	12·9731	13·4043	14·5067	14·7443
	15	10·1477	10·6513	10·7945	11·3975	12·9468	13·3994	14·5033	14·6014

modes and even smaller for the fundamental modes. It is then concluded that sufficient convergence has been achieved for $p = 15$. Hence, this value has been adopted in all examples. It is also worth noting that, with increasing stacking angles, the fundamental frequencies increase monotonically for the circular perforated laminates but decrease for the cantilever, perforated, trapezoidal laminates.

To demonstrate the accuracy and applicability of the present method, the results obtained by the present method have been compared with solutions available in the literature. The example considered was the isotropic, free super-elliptical perforated plates of Material 2, with varying length-to-thickness ratios ($a/h = 1000$, 20, and 4), $a/b = 1$, $a'/a = 0{\cdot}3$, and $b'/a' = 1{\cdot}0$. In Table 3, the finite element solutions based on the three-dimensional elasticity theory using $8 \times 8 \times 4$ terms [19] and the

TABLE 2

Convergence of degree of polynomials p on the frequency parameters λ of the cantilever trapezoidal laminates with free concentric circular hole ($a/b = 2$, $c/b = 0{\cdot}6$, $a'/a = 0{\cdot}3$, *and* $a/h = 5$)

		Mode sequence number							
θ	p	1	2	3	4	5	6	7	8
0	8	1·3319	1·6956	1·8811	4·2521	4·6187	4·8979	7·7518	7·9124
	11	1·3316	1·6949	1·8806	4·2505	4·6171	4·8967	7·7379	7·8878
	13	1·3313	1·6943	1·8803	4·2493	4·6162	4·8962	7·7287	7·8841
	14	1·3312	1·6939	1·8801	4·2487	4·6156	4·8959	7·7230	7·8820
	15	1·3311	1·6937	1·8799	4·2480	4·6153	4·8958	7·7179	7·8806
30	8	0·9375	2·1843	3·0119	3·3024	6·4854	6·9619	7·1355	8·6112
	11	0·9337	2·1677	3·0067	3·2996	6·4807	6·9244	7·1286	8·5716
	13	0·9324	2·1625	3·0049	3·2986	6·4783	6·9112	7·1263	8·5593
	14	0·9319	2·1602	3·0036	3·2981	6·4779	6·9063	7·1254	8·5533
	15	0·9314	2·1580	3·0025	3·2976	6·4774	6·9010	7·1245	8·5478
45	8	0·5763	1·1960	2·4438	3·0481	3·9230	5·2681	5·3150	7·0006
	11	0·5716	1·1811	2·4366	3·0398	3·8995	5·2545	5·2630	6·9880
	13	0·5699	1·1762	2·4339	3·0371	3·8902	5·2345	5·2618	6·9836
	14	0·5692	1·1744	2·4331	3·0357	3·8869	5·2264	5·2616	6·9820
	15	0·5686	1·1727	2·4325	3·0342	3·8834	5·2195	5·2613	6·9811
60	8	0·3870	0·8355	1·8486	2·7816	2·8352	3·7260	4·2173	6·6002
	11	0·3846	0·8299	1·8419	2·7688	2·8275	3·7021	4·2087	6·5837
	13	0·3839	0·8279	1·8395	2·7649	2·8253	3·6935	4·2065	6·5789
	14	0·3836	0·8272	1·8386	2·7633	2·8243	3·6906	4·2059	6·5771
	15	0·3833	0·8266	1·8380	2·7620	2·8232	3·6878	4·2053	6·5760
90	8	0·3143	0·6717	1·5294	1·5692	2·3688	2·5409	3·6905	3·9127
	11	0·3142	0·6716	1·5261	1·5678	2·3682	2·5405	3·6856	3·9035
	13	0·3142	0·6715	1·5250	1·5671	2·3677	2·5403	3·6846	3·9003
	14	0·3141	0·6714	1·5244	1·5668	2·3674	2·5402	3·6842	3·8989
	15	0·3141	0·6714	1·5239	1·5666	2·3672	2·5401	3·6837	3·8982

Rayleigh–Ritz solutions using classical theory using 10×10 terms [21] have been included for comparison. Close agreement is seen between the lowest eight frequencies obtained by the present method and Young's solutions. The next case investigated was an isotropic super-elliptical plate of Material 2, with eccentric circular hole, CF boundary conditions, $a/b = 1$, $a'/a = 0{\cdot}25$, and $b'/a' = 1{\cdot}0$. The eccentricity of circular hole varies from 0 to 0·3. In Table 4, the frequency results were compared in the form of $\lambda_1 = \sqrt{\lambda}/2$ as given in original papers. As anticipated, the results obtained by the present method are in good agreement with previous solutions [1, 8] where methods derived for the membranes were used. In Table 5, the four-ply, super-elliptical, thin perforated plates, made of Material 3 and

TABLE 3

Comparison of frequency parameters λ for the free, super-elliptical, isotropic perforated plates $a/b = 1$, $a'/a = 0{\cdot}3$, and $b'/a' = 1{\cdot}0$

		Mode sequence number							
n_1	n_2	1	2	3	4	5	6	7	8
				Thin plates					
1	1	19·65	19·66	33·66	49·10	49·10	77·53	77·61	87·15
10	1	12·82	18·11	23·16	34·96	34·97	60·65	60·68	66·58
10	10	12·66	17·86	23·05	34·83	34·87	59·93	59·96	67·09
∞	1	12·67	18·11	22·89	34·54	34·55	60·25	60·29	65·78
Reference [19]		12·64	18·06	22·38	32·25	34·25	57·79	57·79	65·52
Reference [21]		12·64	18·08	22·43	34·26	34·26	57·93	57·93	65·62
∞	10	12·51	17·86	22·77	34·42	34·45	59·58	59·63	66·32
∞	∞	12·51	17·86	22·77	34·42	34·45	59·57	59·63	66·32
				$a/h = 20$					
∞	1	12·32	17·91	22·53	33·37	33·38	57·56	57·60	62·46
Reference [19]		12·26	17·81	22·17	33·08	33·08	55·39	55·39	62·38
				$a/h = 4$					
∞	1	10·16	15·04	18·79	23·74	24·80	24·82	25·65	34·97
Reference [19]		10·03	14·93	18·60	22·84	24·53	24·63	24·63	34·88

TABLE 4

Comparison of frequency parameters $\lambda_1 = \sqrt{\lambda}/2$ for the eccentric annular, isotropic plates with CF boundary conditions $a/b = 1$, $a'/a = 0{\cdot}25$, and $b'/a' = 1{\cdot}0$

		Mode sequence number							
d/a	Sources	1	2	3	4	5	6	7	8
0	Reference [1]	3·19	4·60	4·60	5·66	5·88	6·67	6·86	—
	Reference [8]	3·29	4·34	4·34	5·61	5·62	6·84	6·91	7·46
	Present	3·29	4·55	4·55	5·78	5·78	6·82	7·06	7·71
0.075	Reference [1]	3·16	—	4·69	—	5·66	6·32	—	—
	Reference [8]	3·28	4·35	4·39	5·62	5·61	6·60	6·89	7·03
	Present	3·27	4·54	4·64	5·80	5·82	6·43	7·06	7·06
0.15	Reference [1]	3·15	—	4·74	—	5·74	5·97	—	—
	Reference [8]	3·26	4·37	4·46	5·59	5·65	6·29	6·81	7·38
	Present	3·25	4·52	4·81	5·78	6·04	6·22	7·04	7·67
0.225	Reference [1]	3·15	—	4·78	—	5·79	5·97	—	—
	Reference [8]	3·24	4·42	4·53	6·05	5·79	6·10	7·21	8·02
	Present	3·22	4·55	4·75	5·84	6·08	6·27	7·07	7·71
0.3	Reference [1]	3·13	—	4·80	—	5·66	6·30	—	—
	Reference [8]	3·23	4·52	4·43	5·82	—	6·27	7·30	7·97
	Present	3·18	4·57	4·66	5·84	6·02	6·36	7·08	7·75

TABLE 5

Comparison of frequency parameters λ for the four-ply, super-elliptical, E-glass/epoxy, perforated plates with $a/b = 1$, $a'/a = 0{\cdot}3$, and $b'/a' = 1{\cdot}0$

			Mode sequence number							
BC	n_1	n_2	1	2	3	4	5	6	7	8
SF	1	1	14·994	38·350	46·741	73·943	76·641	117·37	119·09	122·07
	Reference [22]		14·979	37·523	44·762	73·572	76·094	116·36	118·26	122·24
	1	10	14·990	38·020	45·896	73·707	76·231	116·74	118·32	127·44
	1	∞	14·990	38·020	45·896	73·706	76·231	116·74	118·31	127·44
	10	1	16·246	36·008	41·936	60·293	71·975	93·240	94·685	107·36
	Reference [22]		16·056	35·426	40·923	60·002	71·607	92·932	93·322	106·47
	10	10	16·394	35·869	41·551	60·117	72·033	94·244	95·722	106·86
	Reference [22]		16·255	35·096	40·090	59·458	71·775	93·053	96·340	105·85
	10	∞	16·394	35·869	41·551	60·117	72·033	94·243	95·724	106·85
	∞	1	16·291	36·143	42·197	60·478	71·936	93·532	94·700	107·37
	Reference [22]		16·190	35·291	40·578	60·259	71·572	93·055	93·359	106·67
	∞	10	16·445	36·015	41·846	60·251	71·984	94·265	96·063	106·83
	Reference [22]		16·377	34·987	39·770	59·606	71·687	92·974	96·820	106·10
	∞	∞	16·445	36·015	41·845	60·251	71·984	94·265	96·065	106·83
CF	1	1	37·177	60·003	69·729	101·82	105·19	149·89	151·90	169·02
	Reference [22]		37·307	59·026	67·610	101·03	104·03	148·97	151·17	169·06
	1	10	38·496	60·113	68·991	101·54	104·75	149·51	150·92	176·63
	1	∞	38·497	60·114	68·992	101·54	104·75	149·51	150·92	176·64
	10	1	31·971	53·711	62·184	82·584	96·389	121·70	127·43	136·45
	Reference [22]		31·827	52·612	60·357	82·079	95·712	120·14	127·06	135·55
	10	10	32·927	53·765	61·649	82·587	96·465	121·06	130·83	135·67
	Reference [22]		33·157	52·471	59·432	81·523	95·889	119·82	131·50	134·49
	10	∞	32·928	53·766	61·649	82·587	94·465	121·06	130·83	135·67
	∞	1	31·758	53·150	61·215	82·187	95·910	120·66	126·95	135·81
	Reference [22]		31·792	51·742	58·611	81·711	95·116	118·88	126·80	135·03
	∞	10	32·689	53·143	60·372	81·852	95·919	120·06	130·37	135·06
	Reference [22]		33·072	51·719	57·904	80·879	95·014	118·78	131·22	133·97
	∞	∞	32·690	53·144	60·372	81·852	95·919	120·06	130·37	135·06

with stacking sequence $[-30/30]_s$, $a/b = 1$, $a'/a = 0{\cdot}3$, and $b'/a' = 1{\cdot}0$ were investigated. Two types of boundary constraints, i.e., SF and CF, have been considered for the laminates. The results from Lim *et al.* [22] obtained by the *p*-Ritz method and classical theory are very close to the present solutions. From the results in Table 5, it is found that stiffer boundary constraints for the outer periphery result in higher frequencies for free vibration. Also, for all cases except circular laminates, higher values for n_2 lead to higher fundamental frequencies. Further, the fundamental frequencies increase for laminated plates subject to SF boundary constraints but decrease for those subject to CF boundary constraints when n_1 is increased. It is worth addressing that the results for $n = \infty$ were obtained by assuming a rectangular laminate rather than a super-elliptical laminate with much

TABLE 6

Comparison of frequency parameters λ *for the rectangular laminates with* $a = 448$ mm, $b = 114$ mm, *and stacking sequence* $[45/0/0/90/0/-45/0]_s$

Boundary conditions		Mode sequence number							
		CSCS				CSCF			
a' (mm)	Sources	1	2	3	4	1	2	3	4
0	Reference [23]†	26·097	32·960	41·969	53·909	6·006	12·655	22·522	30·958
	Reference [23]‡	21·950	28·242	38·823	53·623	5·720	13·942	25·668	30·172
	Present	21·950	28·170	38·752	53·552	6·006	14·800	27·312	32·031
22	Reference [23]†	20·877	26·740	34·962	47·045	5·934	12·655	22·665	28·599
	Reference [23]‡	21·592	28·242	38·323	53·552	5·720	13·871	25·453	29·529
	Present	21·950	28·170	38·752	53·552	6·006	14·800	27·312	31·959
35	Reference [23]†	20·877	27·598	36·249	47·689	6·292	13·585	24·810	28·599
	Reference [23]‡	21·378	28·099	38·251	52·837	5·720	13·799	25·382	29·028
	Present	21·950	28·170	38·823	53·552	6·006	14·800	27·312	31·888
44	Reference [23]†	22·450	27·455	38·394	47·117	5·291	13·513	25·167	29·314
	Reference [23]‡	21·235	27·241	38·466	51·979	5·720	13·728	25·130	28·671
	Present	21·878	28·170	38·823	53·552	6·077	14·800	27·312	31·745
57	Reference [23]†	20·806	26·383	32·531	43·185	6·292	12·369	22·450	29·314
	Reference [23]‡	21·306	27·527	39·252	50·191	5·791	13·585	25·310	28·313
	Present	21·807	28·170	38·823	53·552	6·077	14·729	27·312	31·530

† Experimental result.
‡ Finite element method and classical laminated plate theory.

higher n. Table 6 gives a comparison of non-dimensional frequency results for the rectangular, thin, perforated laminates with a concentric free circular hole, $a = 448$ mm, $b = 114$ mm, stacking sequence $[45/0/0/90/0/-45/0]_s$, and made of Material 4. The diameter of hole a' varies from 0 to 57 mm and the outer periphery of plates were subject to CSCS and CSCF boundary conditions. It is seen that the frequency parameters obtained by the present method and those of the finite element method [23] agree moderately for the lowest four modes.

Because both the inner and outer boundaries of the perforated plates can be described by the super-elliptical equations, it is interesting to study the change in the super-elliptical powers for the lowest eight frequencies of the laminated plates. In Table 7, two types of completely free perforated laminates with $a/b = 1$, $a'/a = 0{\cdot}3$, $a'/b' = 1$, and $[(45/-45)_2]_s$ have been studied. The first type is the laminate with a concentric circular hole and the super-elliptical power n_1 varies from 1 to infinity. The second type represents a circular perforated laminate with a concentric super-elliptical hole and the super-elliptical power n_2 increases from

TABLE 7

Lowest eight frequency parameters λ for the super-elliptical laminated perforated plates with FF boundary conditions, $a/b = 1$, $a'/a = 0{\cdot}3$, $a'/b' = 1$, and $[(45/-45)_2]_s$

		Mode sequence number							
n_1	n_2	1	2	3	4	5	6	7	8
1	1	3·6905	7·5741	7·8715	10·7022	11·2893	11·4458	13·5638	13·9774
2	1	3·6481	5·9669	7·6065	8·6619	9·2654	9·8424	12·1182	12·6223
3	1	3·6524	5·5535	7·5786	8·0906	8·7292	9·3783	11·7686	12·2715
4	1	3·6568	5·3830	7·5705	7·8401	8·5011	9·1793	11·6262	11·9938
5	1	3·6595	5·2961	7·5669	7·7072	8·3813	9·0742	11·5551	11·8477
6	1	3·6612	5·2458	7·5649	7·6284	8·3103	9·0117	11·5145	11·7620
7	1	3·6622	5·2141	7·5636	7·5779	8·2647	8·9714	11·4892	11·7076
8	1	3·6629	5·1930	7·5438	7·5627	8·2337	8·9440	11·4724	11·6708
9	1	3·6633	5·1782	7·5198	7·5621	8·2116	8·9244	11·4607	11·6449
10	1	3·6636	5·1674	7·5023	7·5616	8·1953	8·9100	11·4522	11·6258
20	1	3·6644	5·1326	7·4454	7·5598	8·1402	8·8611	11·4252	11·5619
40	1	3·6645	5·1243	7·4327	7·5594	8·1256	8·8483	11·4196	11·5448
∞	1	3·6707	5·1534	7·4890	7·6161	8·1612	8·8748	11·4885	11·5329
1	2	3·6338	7·3050	7·4781	10·4554	10·9444	11·3387	13·0499	13·7624
1	3	3·6221	7·2445	7·4043	10·4056	10·8678	11·3100	12·9987	13·7175
1	4	3·6176	7·2239	7·3773	10·3903	10·8391	11·2991	12·9841	13·7021
1	5	3·6155	7·2149	7·3647	10·3844	10·8259	11·2940	12·9784	13·6954
1	6	3·6144	7·2104	7·3581	10·3817	10·8189	11·2913	12·9757	13·6921
1	7	3·6137	7·2079	7·3542	10·3802	10·8148	11·2897	12·9743	13·6903
1	8	3·6133	7·2064	7·3518	10·3794	10·8123	11·2888	12·9734	13·6891
1	9	3·6130	7·2054	7·3503	10·3789	10·8107	11·2882	12·9729	13·6884
1	10	3·6128	7·2047	7·3493	10·3786	10·8096	11·2877	12·9726	13·6880
1	20	3·6124	7·2033	7·3469	10·3778	10·8072	11·2868	12·9718	13·6869
1	30	3·6124	7·2032	7·3468	10·3778	10·8071	11·2867	12·9718	13·6869
1	40	3·6124	7·2032	7·3468	10·3778	10·8070	11·2867	12·9718	13·6869

1 to 40. Based on the results shown in Table 7, it is found that all modes except the fundamental modes of the first type laminates decrease with the increase of super-elliptical powers n_1 or n_2. The increase in super-elliptical power n_1 or n_2 leads to the increase in mass and therefore the decrease in the frequencies. However, for the fundamental modes of super-elliptical perforated laminates with $n_1 > 1$ and a concentric circular hole, a different trend is seen where higher fundamental frequencies were obtained for higher n_1.

In the rest of the examples, we investigated thick perforated laminates with different geometries as described in Figure 3. Variation of the frequencies with respect to the stacking angle θ as well as super-elliptical powers n_1 and n_2 of the super-elliptical, perforated laminates are given in Table 8 and Figure 4. In Table 8, we examined the super-elliptical laminated plates with concentric circular hole, $a/b = 1$, subject to FF boundary conditions as described in Figure 3(a). It is

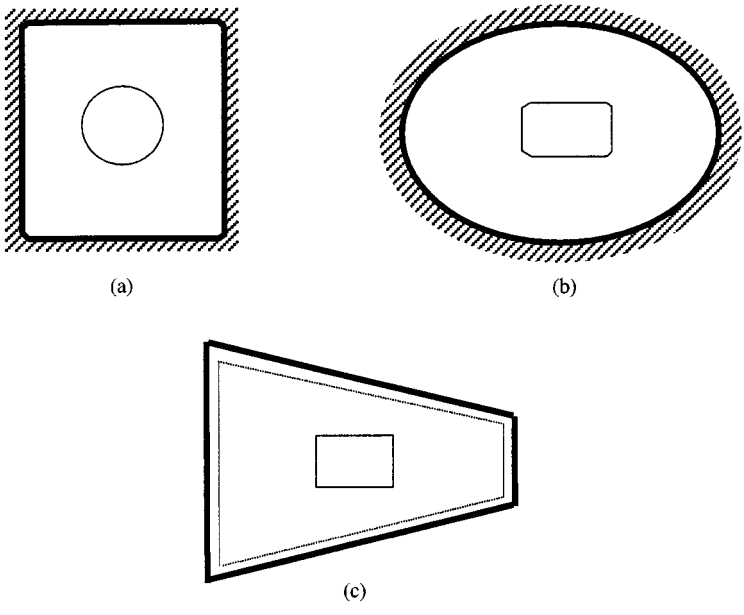

Figure 3. Geometric definitions of the laminated perforated plates considered for the numerical studies.

TABLE 8

Lowest eight frequency parameters λ for the super-elliptical laminated perforated plates with FF boundary conditions, $a/b = 1$, $a'/a = 0{\cdot}3$, $a'/b' = 1$

			Mode sequence number							
n_1	n_2	θ	1	2	3	4	5	6	7	8
1	1	0	3·4601	3·5038	6·8985	7·6255	7·6520	7·9961	10·1925	10·2810
		15	3·5680	5·4136	8·1729	8·7197	9·6698	11·2159	11·8685	12·0306
		30	3·6341	6·9539	8·5242	9·6678	10·6548	11·3481	12·3733	14·3591
		45	3·6905	7·5741	7·8715	10·7022	11·2893	11·4458	13·5638	13·9774
10	1	0	2·2450	2·9579	5·1936	6·2653	7·1838	7·4823	7·5391	9·1017
		15	3·0361	3·7161	7·0222	7·4885	7·7768	7·9604	10·0698	10·8633
		30	3·3444	4·8530	7·9477	7·9685	8·6106	8·6428	8·7966	10·8005
		45	3·6636	5·1674	7·5023	7·5616	8·1953	8·9100	11·4522	11·6258
∞	1	0	2·2196	2·9429	5·1295	6·2584	7·1587	7·4689	7·4760	8·9965
		15	3·0206	3·6854	6·9576	7·4668	7·7583	7·8848	10·0038	10·8859
		30	3·3346	4·8178	7·8821	7·9594	8·5939	8·6076	8·7166	10·6856
		45	3·6707	5·1534	7·4890	7·6161	8·1612	8·8748	11·4885	11·5329

observed that the fundamental frequencies increase monotonically as the stacking angles increase. Similar trends as previous examples are seen where an increase in super-elliptical power n_1 leads to a decrease in frequencies. As expected, frequency results for the super-elliptical perforated laminate with $n_1 = 10$ and rectangular

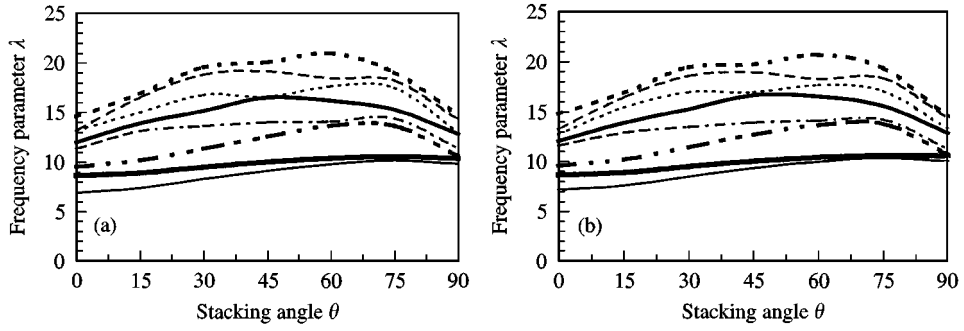

Figure 4. Lowest eight frequency parameters λ for the elliptical, perforated laminates with CF boundary condition, $a/b = 2$, $a'/a = 0{\cdot}3$, $a'/b' = 1$, and stacking sequence $[(\theta/-\theta)_2]_s$. (a) $n_2 = 1$; (b) $n_2 = 10$. ——, 1; ——, 2; — -, 3; –·–·, 4; ——, 5; ----, 6; – – –, 7; ---, 8.

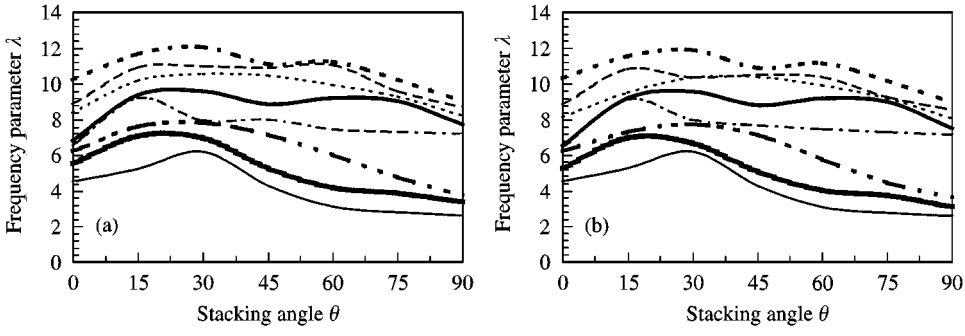

Figure 5. Lowest eight frequency parameters λ for the trapezoidal, perforated laminates with SF boundary condition, $a/b = 2$, $c/b = 0{\cdot}6$, $a'/a = 0{\cdot}3$, $a'/b' = 1$, and stacking sequence $[(\theta/-\theta)_2]_s$. (a) $n_2 = 1$; (b) $n_2 = \infty$. ——, 1; ——, 2; — -, 3; –·–·, 4; ——, 5; ----, 6; – – –, 7; ---, 8.

perforated laminates are very close because of the similarity in their peripheries. In Figure 4, the super-elliptical laminated perforated plates with CF constraints, $a/b = 2$, $a'/a = 0{\cdot}3$, $a'/b' = 1$, and stacking sequence $[(\theta/-\theta)_2]_s$ were considered. The holes were assumed to be circles or super-ellipses with $n_2 = 10$ as shown in Figure 3(b). A cursory examination of the lowest eight frequencies shown in Figure 4(a, b) reveals that maximum frequencies are likely to appear if the stacking angle is between 45 and 75°. Next we examined the thick, trapezoidal, perforated laminates of Material 1 with SF boundary conditions, $a/b = 2$, $c/b = 0{\cdot}6$, $a'/a = 0{\cdot}3$, $a'/b' = 1$, $a/h = 5$, stacking sequence $[(\theta/-\theta)_2]_s$, and with a circular or rectangular hole as seen in Figure 3(c). From the results in Figure 5(a, b), it is seen that maximum frequencies were obtained for a stacking angle between 15 and 60°. It is found that the fundamental frequencies increase slightly for the perforated laminates with a square hole at the center of the plate. In Table 9, the eccentric, annular laminates of Material 1, with CF boundary condition, $a'/a = 0{\cdot}3$, and stacking sequence $[(\theta/-\theta)_2]_s$ were investigated. The eccentricity d/a of the circular hole was increasing from 0 to 0·3. It is noted that maximum fundamental frequencies appear

TABLE 9

Lowest eight frequency parameters λ for the eccentric, annular perforated laminates with CF boundary condition and $a'/a = 0{\cdot}3$

		Mode sequence number							
d/a	θ	1	2	3	4	5	6	7	8
0	0	8·4096	9·6607	12·2738	12·5419	14·1889	14·6003	15·2910	16·4064
	15	8·5361	10·1700	12·4929	15·0273	15·7417	18·6467	19·4684	19·5351
	30	8·8650	11·2126	12·3198	16·1965	17·2450	20·1362	22·3831	22·4932
	45	8·9766	11·7128	12·1041	16·5033	18·2287	20·9470	22·0885	22·8164
0·1	0	7·9442	9·6270	11·8875	13·0273	15·3338	15·5396	15·6868	16·4414
	15	8·0985	10·1319	13·3014	15·5631	16·0841	18·7062	19·0024	19·4804
	30	8·4540	11·2208	13·4182	16·2451	17·6613	19·7488	21·8854	22·5640
	45	8·6483	11·9578	12·9462	16·4161	18·2759	19·9581	21·7838	22·8943
0·2	0	7·6752	9·4943	11·8123	13·0881	15·6860	15·9647	16·2967	17·1014
	15	7·8709	9·9769	13·5657	15·7663	16·6873	18·3656	19·1018	21·3770
	30	8·2722	11·0072	14·1865	16·1150	18·1553	20·7278	21·9770	22·5095
	45	8·5398	11·7089	13·8993	16·1653	19·1625	19·8032	21·6472	24·2451
0·3	0	8·1383	9·1647	12·4667	13·1968	15·0235	15·4950	16·1687	16·9064
	15	8·3556	9·6048	13·5524	15·5579	16·8273	18·6619	19·2179	20·8636
	30	8·7888	10·4248	13·8523	15·8651	18·6022	21·5428	21·7075	22·2982
	45	9·0415	10·9736	13·5252	15·7991	19·3409	20·5956	21·8909	25·2669

when the stacking angle is 45°. However, the effect of the eccentricity of the hole on the frequencies of the thick annular laminated plates considered herein is irregular.

4. CONCLUSIONS

In this paper, the natural frequencies of symmetrically laminated, thick, perforated plates have been obtained using the Rayleigh–Ritz method by employing Reddy's higher order plate deformation theory. The laminates were subject to a variety of aspect ratios, length-to-thickness ratios, super-elliptical powers, stacking angles, and boundary conditions.

Some important conclusions can be drawn as shown below:

(1) Generally, the frequency parameters decrease with increasing length-to-thickness ratios or super-elliptical powers n_1 and n_2, although for some cases the boundary constraints should be taken into account as well.
(2) Stiffer boundary constraints for the outer periphery result in higher frequencies.
(3) The similarity between the geometries of super-elliptical power $n = 10$ and the rectangle ($n = \infty$) leads to close frequency results for both planforms.

(4) The variations of frequencies for circular laminates with concentric and eccentric holes are irregular.

REFERENCES

1. K. Nagaya 1977 *ASME Journal of Applied Mechanics* **44**, 165–166. Transverse vibration of a plate having an eccentric inner boundary.
2. K. Nagaya 1977 *Journal of Sound and Vibration* **50**, 545–551. Vibration of membrane having a circular outer boundary and an eccentric circular inner boundary.
3. K. Nagaya 1981 *Journal of Sound and Vibration* **74**, 543–551. Simplified method for solving problems of vibrating plates of doubly connected arbitrary shape. Part I: derivation of the frequency equation.
4. K. Nagaya 1981 *Journal of Sound and Vibration* **74**, 553–564. Simplified method for solving problems of vibrating plates of doubly connected arbitrary shape. Part II: applications and experiments.
5. G. S. Sarmiento, P. A. A. Laura and R. H. Gutierrez 1984 *Journal of Sound and Vibration* **93**, 585–587. Comments on "free transverse vibrations of uniform circular plates and membranes with eccentric holes".
6. R. H. Gutierrez and P. A. A. Laura 1997 *Journal of Sound and Vibration* **201**, 133–136. Transverse vibrations of square membrane with an eccentric circular or quasi-square hole.
7. H. B. Khurasia and S. Rawtani 1978 *ASME Journal of Applied Mechanics* **45**, 215–217. Vibration analysis of circular plate with eccentric hole.
8. W. H. Lin 1982 *Journal of Sound and Vibration* **81**, 425–435. Free transverse vibrations of uniform circular plates and membranes with eccentric holes.
9. J. G. Tseng and J. A. Wickert 1994 *ASME Journal of Vibration and Acoustics* **116**, 155–160. Vibration of an eccentricity clamped annular plate.
10. A. Rajamani and R. Prabhakaran 1977 *Journal of Sound and Vibration* **54**, 549–564. Dynamic response of composite plates with cut-outs. Part I: simply-supported plates.
11. A. Rajamani and R. Prabhakaran 1977 *Journal of Sound and Vibration* **54**, 565–577. Dynamic response of composite plates with cut-outs. Part II: clamped–clamped plates.
12. K. M. Liew 1993 *International Journal of Solids and Structures* **30**, 337–347. Treatments of over-restrained boundaries for doubly connected plates of arbitrary shape in vibration analysis.
13. C. W. Lim and K. M. Liew 1995 *ASCE Journal of Engineering Mechanics* **121**, 203–213. Vibration of perforated plates with rounded corners.
14. P. C. Yang, C. H. Norris, and Y. Stavsky 1966 *International Journal of Solids and Structures* **2**, 665–684. Elastic wave propagation in heterogeneous plates.
15. J. N. Reddy 1984 *ASME Journal of Applied Mechanics* **51**, 745–752. A simple higher order theory for laminated composite plates.
16. A. S. Bicos and G. S. Springer 1989 *International Journal of Solids and Structures* **25**, 129–149. Analysis of free damped vibration of laminated composite plates and shells.
17. A. S. Bicos and G. S. Springer 1989 *AIAA Journal* **27**, 1116–1121. Vibrational characteristics of composite panels with cutouts.
18. S. Ramkrishna, K. M. Rao and N. S. Rao 1993 *Computers and Structures* **47**, 281–287. Dynamic analysis of laminates with elliptical cutouts using the hybrid-stress finite element.
19. P. G. Young, J. Yuan and S. M. Dickinson 1996 *ASME Journal of Vibration and Acoustics* **118**, 184–189. Three-dimensional analysis of the free vibration of thick rectangular plates with depressions, grooves or cut-outs.
20. K. M. Liew and C. M. Wang 1993 *Engineering Structures* **15**, 55–60. *pb*-2 Rayleigh–Ritz method for general plate analysis.

21. P. G. YOUNG and S. M. DICKINSON 1993 *Journal of Sound and Vibration* **165**, 511–526. On the free vibration of thin isotropic and rectangularly orthotropic plates involving curved boundaries.
22. C. W. LIM, S. KITIPORNCHAI and K. M. LIEW 1998 *Composite Sciences and Technology* **58**, 435–445. Free vibration analysis of doubly connected super elliptical laminated composite plates.
23. G. B. CHAI 1997 *Composite Structures* **35**, 357–368. Free vibration of laminated composite plates with a central circular hole.